

MASTER

UCRI-85287
PREPRINT

CONF-YIC-12-24

CONFIGURING THE THERMOCHEMICAL HYDROGEN
SULFURIC ACID PROCESS STEP FOR
THE TANDEM MIRROR REACTOR

Terry R. Galloway

This paper was prepared for submittal to
1981 Intersociety Energy Conversion Engineering
Conference, Atlanta, Georgia, August 9-14, 1981

May 1, 1981

This is a preprint of a paper intended for publication in a journal or proceedings. Since changes may be made before publication, this preprint is made available with the understanding that it will not be cited or reproduced without the permission of the author.



Lawrence
Livermore
Laboratory

DISTRIBUTION OF THIS DOCUMENT IS UNLIMITED

Configuring the Thermochemical Hydrogen Sulfuric Acid
Process Step for the Tandem Mirror Reactor

Terry R. Galloway
Lawrence Livermore National Laboratory
Livermore, California 94550

ABSTRACT

In joint program* between University of Washington, the General Atomic Company and ourselves, we are developing a conceptual "point design" for a Tandem Mirror Reactor-driven thermochemical hydrogen plant.

This paper identifies the sulfuric acid step as the critical part of the thermochemical cycle in dictating the thermal demands and temperature requirements of the heat source. We couple the General Atomic Sulfur-Iodine Cycle to a Tandem Mirror Reactor.

We focus specifically on the sulfuric acid decomposition process step since this step can use the high efficiency electrical power of the direct converter together with other thermal-produced electricity to Joule-heat a non-catalytic SO_3 decomposer to approximately 1250 K. This approach uses concepts originally suggested by Dick Werner and Oscar Krikorian. The blanket temperature can be lowered to about 900 K, greatly alleviating materials problems, the level of technology required, safety problems, and costs.

We have used a moderate degree of heat integration to keep the cycle efficiency around 40%, but limited the number of heat exchangers in order to keep hydrogen production costs within reasonable bounds.

INTRODUCTION

A projection of the energy supply and demand picture beyond the turn of the century shows (1) a substantial role for fusion both in the generation and in the production of synthetic fuels--starting with hydrogen.

Hydrogen, already a valuable raw material for our large U.S. petro-chemical and petrochemical industries, by early 2000 is expected to become an important renewable-based transportable fuel by itself or in some hydrocarbon form, such as methanol. Hydrogen can be produced through decomposition of water by means of thermochemical cycles, which reduce the high temperature 3000 K requirements of the straight thermal decomposition process to thermal levels that can be generated in nuclear fission or fusion reactors, or in high intensity, focused solar collectors.

We have been studying the interfacing of our Tandem Mirror Fusion Reactor (TMF) to several thermochemical cycles under a DOE contract at LLNL entitled: "Synfuels from Fusion" (2). In this program we take advantage of the favorable engineering features of the TMF configuration. The TMF consists of a cylindrical solenoidal, energy-producing section between end cells that provide the containment; the solenoid contains modular blanket sections with simple piping and electrical connections. The blanket produces heat. The direct converter produces both electricity and heat as the result of ion leakage out of the plasma into the end cells. The

required tritium to fuel the DT reactor is also generated in the blanket modules. Materials and engineering structural problems are minimized by the favorable geometry, the steady state magnetic field and the temperature.

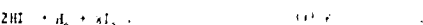
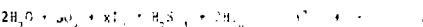
The chemical engineering portion of our program plan on this project is to develop a process design which is simple and credible, to keep the overall temperature requirement as low as possible, and to utilize the unique advantages that fusion deuterium offers as drivers to thermochemical hydrogen initiatives.

In his portion of the study, Dick Werner shows the approximately 400 K conversion temperature when the liquid metal such as a lithium-uranium eutectic alloy is a large number of small modules which surround the cylindrical plasma, and heat passes directly from the heat from the liquid metal out into the plasma.

The higher grade energy needed for the high-temperature SO_3 decomposition process step is about 1000 K, is supplied not from the blanket, but from the reactor, but, as initially proposed by R. Werner (3), the conversion efficiency via tritium breeding is only small quantities. In the TMF direct converter, the tritium is heated by the SO_3 decomposer. In addition, in Ref. (3) we developed the conceptual design for a catalyzed bed SO_3 decomposer (3), the heat of which was supplied entirely from the blanket; thus, raising the reactor temperature up to 1200 K. This is a large amount of Joule heated electrical energy, as well as a large increase in the blanket temperature, about 300 K.

Sulfur-Iodine Cycle Design

The sulfur-iodine cycle design, developed by the General Atomic Company (4), is a pure thermochemical type operating in an all-catalytic mode. In addition, the essential steps of the SO₂ conversion are as follows:



All reactions in this system have been verified in the laboratory and total cycle has been demonstrated in a closed loop cyclic, small-scale demonstration. None of these reactions goes to completion; therefore, it is necessary to separate reaction products from the reactants. Major parts of the process are associated with separation and purification of the reaction products. A key to the successful operation of the process is the liquid-liquid phase separation of the reaction products of reaction (1). These solutions are separated into a lower density phase, containing H_2SO_4 and H_2O , and a higher density phase containing HI , I_2 , and H_2O . This important advancement was developed at General Atomic.

Figure 1 is a schematic flow diagram of the sulfur-iodine cycle showing product mass flow and the recycle streams. The features shown in the conceptual block diagram in Fig. 1, are adequate for this paper.

In general, flowsheets of Section I involve H_2SO_4 and HI Production and Separation; Section II, H_2O_2

*This work was performed under the auspices of the U.S. Department of Energy by Lawrence Livermore National Laboratory under contract No. W-7405-Eng-48.

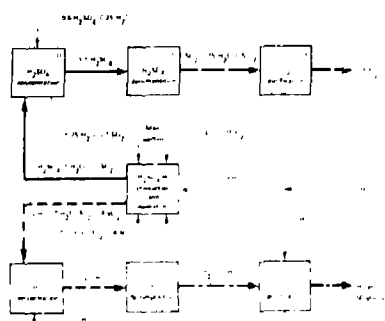


Fig. 10. Simplified schematic flow diagram of surface piping system (Courtesy General Atomic Company).

Concentration and use, see Appendices, Section III, III
 Separation, see I, II, III, Decomposition and II
 Preparation, see I. The following heat load for the
 preparation of the samples was used: 600 °C for 10 min. In
 the case of the samples with 10% and 20% of Fe_2O_3 the
 heat load was increased to 650 °C for 10 min.

THE VENUS OF WILLISTON

On 11 January 1975 between the Tandem Mirror Reactor and the experimental D₃ system in Fig. 2, the two steps are required of William's to make the process start. In this case the low temperature process steps of the two steps are carried over 144 of the TMR energy steps, and 491 of the D₃ system's electricity from

We have now examined the engineering and safety aspects of the moderating cycle by means of the more conservative elements. Liquid lithium coolants and associated elements of the breeder unit and steam generation. The present conceptual design appears to be in the direction of a safe and reliable

784 *Environ Biol Fish* (2004) 67

The data presented in the No. 1 deactivation report were obtained at Westinghouse (6), the Nuclear Research Division, Argonne, Illinois, by General Atomics in San Diego, California, but the work center at Kepro, Inc., was the temperature effect of temperature and pressure on the NO_x/SO_2 equilibrium in the presence of water vapor, available (10) and is shown in Fig. 10. The 1 atmosphere reactor exit total

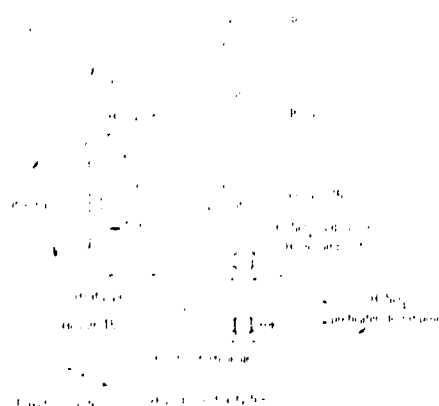


Fig. 2. New concept for coupling the G.A. cycle to the TMR.

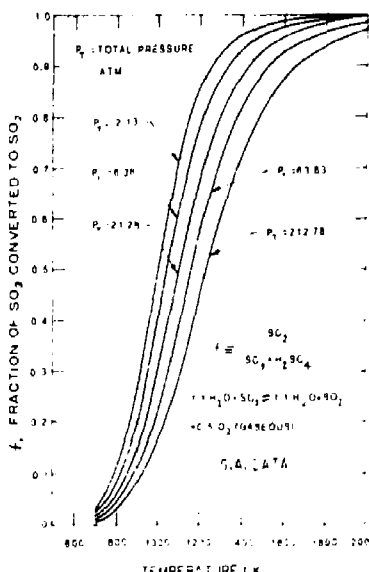


FIG. 3. $\text{SO}_2\text{-SO}_3$ equilibrium in the presence of the TiO_2 (10 wt-%) atomic compound.

pressure and 1250 K, the time for decomposing SO_2 is around 64 s. We have plotted $\ln(1 - \frac{P_{\text{SO}_2}}{P_{\text{SO}_2,0}})$ for the SO_2 decomposition, the results are shown in Figure 10, illustrating the need for a kinetic model to predict the decomposition in the DSC analysis. This comparison is for SO_2 in N_2 at a pressure of 43.5

Chromatography

Now that we have learned the importance of the TMR to the kinetics, we should examine the other kinetics of the system. In order to do this, a better design concept is required. We have attempted to get SO₂ and O₂ at stoichiometric ratios using a Joule-heated element and have obtained a 100% internal heat exchanger system. At 1200 K, the estimated curve in Fig. 4 indicates that 100% alumina alone can provide only 30% conversion. In this area, that no further pressure reduction or more fresh catalyst need be used. Since a庚ting effect was suggested by Oscar Finsen et al.,¹⁰ in our design, as we shall see later, we assume that a庚ting effect will be equally effective as the alumina shown in Fig. 4, and used only 50% alumina.

Fig. 4, and need not be satisfied. There is also the problem of the back reaction of SO_2 and I_2 to SO_3 at 1250 K, as shown in a study by Royner [19], in Fig. 5. Although his study was undertaken for a 2000 K SO_3 decomposer reactor, we believe [12] that his results can be used to estimate our 1250 K SO_3 decomposition case, as shown by the dashed curve in Fig. 5. We expect the conversion to decrease to around 77% owing to a back reaction resulting from a quenching rate of at least 300 K/sec in the cooling heat exchanger following the decomposer. We will discuss this quenching rate later in this paper.

H₂SO₄ Process Step Configuration

We have configured the H_2SO_4 process step in such a way as to keep the blanket at around 900 K and supply all of the thermal energy demand above 900 K from the electrical heating. As shown in Fig. 6 the multi-effect evaporator train is operated between 500

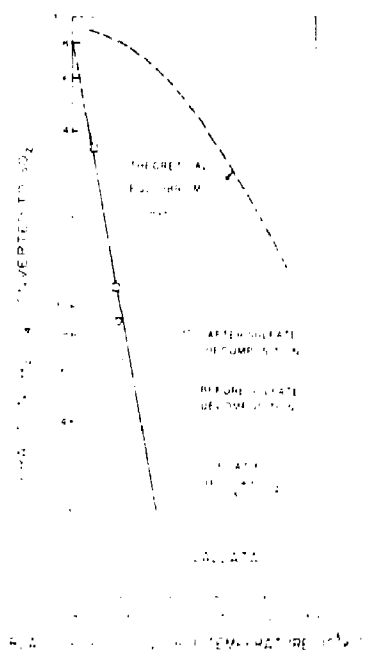


Fig. 4. Sulfuric acid decomposition on alumina substrate (Alma P-1-4-B). (Courtesy General Atomic Company.)

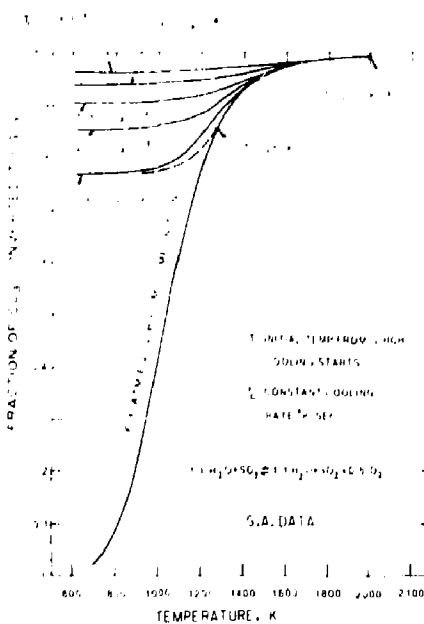


Fig. 5. Back conversion of SO_2 to SO_3 during cool down.



Fig. 6. Configuring the Sulfuric Acid Section for the Joule-Boosted SO_3 Decomposer.

and 600 K the H_2SO_4 is boiled at 600 K, the decomposer preheater is operated from 580 to 350 K and the SO_3 decomposer at 1250 K.

For this process configuration the thermodynamic for the H_2SO_4 - SO_3 - H_2O system can be used to generate an enthalpy-temperature curve as shown in Fig. 7 (15). Note that in the temperature range of 700 to 1050 K no SO_3 decomposition is assumed to have taken place, whereas at 1050 K, as the process gas is passed from the preheater to the decomposer, the SO_3 decomposition in the decomposer is presumed to take place as the gas is heated from 1050 to 1250 K. The kinetic data in Fig. 4 help support this supposition since at a value of $10^3/T = 0.95$ (i.e. 1000 K), only about 3% of the SO_3 is converted to SO_2 .

Our challenge now is to provide heat at the required temperature to the evaporating, boilers and decomposer preheater, and decomposer as shown in Fig. 1, using thermal and electrical energy from the direct converter and from the blanket and first wall. The fraction energy output available for process chemistry as well as the distribution between thermal and electrical energy from the direct converter is shown in Table 1 (2). We desire the lowest value of the TMR γ (ratio of fusion power out to injected power in) such that we can match the energy demands of the complete thermocchemical cycle without raising the blanket temperature above 900 K. This value of γ of 15 gives a total fusion power output level of 3,000 MW_t from the TMR. After electricity is used for neutral beam injectors and ion cyclotron resonance heating, 2688 MW_t is available for the chemical process.

Table 2 summarizes the energy supply and demand. For this case, the overall cyclic efficiency for producing H_2 is calculated as 48.9%. Parametric studies show significant improvements in cycle efficiencies with higher TMR γ and higher input temperatures to the decomposer.

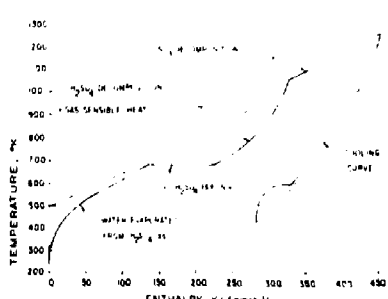


Fig. 7. Enthalpy heating curve for $\text{H}_2\text{SO}_4/\text{H}_2\text{O}$ system.

Table 1. Direct Converter Energy Output Available for Process Chemistry (Injector and Direct Converter $n = 0.60$) Percentage of MW_t.

TMR Q	Blanket	D.C. Thermal	D.C. Elect. To Synfuel
	Thermal	Thermal	To Synfuel
5	95.09	16.00	-11.09
10	88.36	11.21	0.43
15	86.31	9.75	3.93
20	85.32	9.04	5.63
25	84.74	8.63	6.63
30	84.35	8.35	7.30
35	84.08	8.16	7.76
40	83.87	8.01	8.11
50	83.59	7.81	8.60

A longer term fusion goal is to ultimately operate on DD, in which case the particle flux into the direct converter increases from 20% to about 50%, thus increasing substantially the dc electrical power available to the process from 4% to around 30%. This would be sufficient to supply all of the electrical needs of the Joule-boosted decomposer instead of converting thermal energy to ac power with a loss in cycle efficiency.

Joule-Boosted SO₃ Decomposer

Last year we developed conceptual designs for the SO₃ decomposer involving a catalytic packed bed reactor (14-15), a fluidized catalytic bed reactor (3), and the catalytic cartridge heat pipe design (1). All of these design concepts made use of the higher temperature 1200 °F Li-Na cauldron blanket design and made no special use of the unique properties of the direct converter.

The Joule-boosted decomposer is therefore unique, in that it uses electrical energy to heat SiC heating elements (suggested by Krikorian (3) to be commercially available and widely used today and believed by him to be compatible with the decomposing SO₃ vapors). Such a decomposer design is depicted in Fig. 8. Large SiC heating elements, 3/4 cm in diameter and 3.04 m long are arranged vertically with the process gases fed in crossflow. They are coupled to commercial crossflow shell and tube heat exchangers. The ends of these heating elements are passed via insulators through the header sheets and are cooled by a coolant gas down to 600 K. These ends must be cooled in order to provide for the commercial, present-day aluminum impregnated electrical feed connection. The heat loss out the ends of the elements is negligibly small at around 1%.

In developing this design concept, we have sized the vessel and components. The SiC heating elements are proposed to be formed with small corrugations in the surface as shown in Fig. 9, to benefit the gas-solid heat transfer coefficient as we will discuss

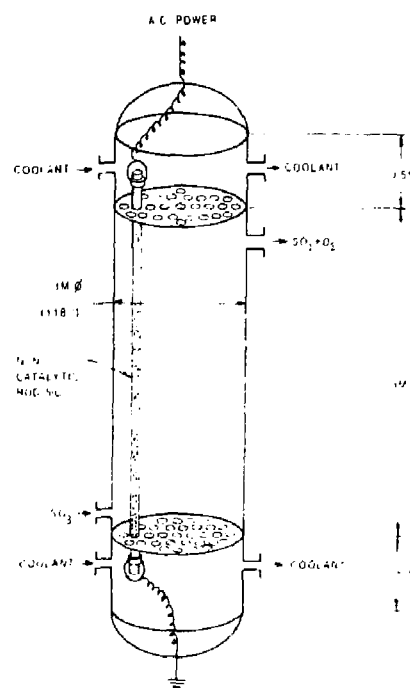


Fig. 8. Joule-Boosted SO₃ Decomposer.

later. These elements are configured in a hexagonal array with a 6.1 cm spacing normal to the flow and 1.3 cm spacing in the flow direction as shown in Fig. 9.

These elements can be operated up to 130 kW_t (80 W/cm²) at 1250 K. However, to achieve the long-life, beyond electrically heated furnaces and kilns, we have selected a λ of 0.8 kW/m² (40 W/cm²). We hope to achieve a 10 year life. At this flux, we need around 17,000 elements with a total extended surface area of 14,330 m² (0.84 m² per element). Using heat transfer correlations for staggered tubes in cross flow (14,15), we find that we can juice this decomposer at a gas to element surface $T = 779$ K. Eight vessels are used. For this configuration the Reynolds number for the process gases flowing cross flow to the SiC heating elements, calculated at the minimum flow cross section is $Re = 300,000$, the Nusselt number is $Nu = 418$, and heat transfer coefficient is $h = 120$ cal/m²·s·K (92 Btu/h·ft²·R). At this rate of flow through

Table 2. Energy Supply and Demand Basis 3,000 MW_t TMR.

Unit	Temp (K)	Process Demand	Process Supplied	TMR Supply Direct Converter	TMR Supply Blanket
SO ₃ Decomposer	950-1250	571 MW _t	0	94.5 MW _e	168 MW _e
Decomp. Preheat.	680-950	720	0	0	0
H ₂ SO ₄ Boiler	580	536	242	0	260
H ₂ SO ₄ Evap.	380-680	773	664	0	109
Decomp. Recuperator	1250-800	0	720	0	0
Decomp. Cooler	800-418	0	1241	0	0
Remaining Units	418-680	702	0	0	702
Pumping Power	-	517	0	0	0

H₂ Product Chemical Energy Produced as Higher Heating Value = 285.2 kJ/gmol H₂.

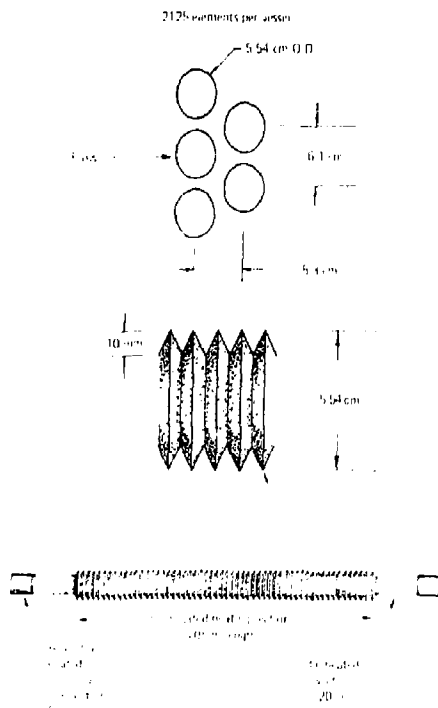


Fig. 9. Silicon carbide heating elements for the SO_3 decomposer.

these eight vessels (i.e., 217 m^3/s), the pressure drop (in-out) would be 10.7 kPa (0.1 atm) and the pumping power is calculated at 23 MW_t total or 60 MW_t for blanket heat converted to electricity at 38% to run the blower.

We have selected this cross flow geometry for the decomposer heating elements because of significant heat transfer advantages. Cross flow around the 5.5 cm diameter elements is more effective (i.e., higher Reynolds and Nusselt number at a lower process velocity) owing to reformation and growth of the boundary layer and the separation and wake formation aft of the cylinder. These wakes provide turbulence which enhance the heat transfer. This heat transfer observation is based on an extensive experimental study (15) of staggered tubes in cross flow and we believe it is reliable.

One approach to estimating the SO_3/O_2 quench rate is to take the residence time of the process gas in the cooler. We assume the gas leaves the decomposer at 1170 K (i.e. 79 K below the 1250 K SiC element temperature) and no back reaction had time to occur as the SO_2 and O_2 is transported away from the SiC surface, through the thermal boundary layer into the gas. The recuperator heat exchanger immediately following the decomposer, we have designed as follows: six crossflow U-tube heat exchangers 2.6 m in diameter, 5 m in height. Operating at an $\text{LMDD} = 139$ K, with an overall heat transfer coefficient of $h = 614 \text{ W/m}^2\text{K}$ (102 $\text{Btu/h}\cdot\text{ft}^2\text{F}$) and a tube surface area of 4500 m^2 . There are about 480 U-tubes per unit which together handle the required 386 MW_t . For this design the quench rate would be 1400 K/s at a residence time of

0.36 s. According to Rovner's Fig. 5, this rapid quench rate would not cause a significant back reaction.

The eight SO_3 decomposer vessels lined inside with insulation can be fabricated out of Incoloy 800H to withstand the 0.7 MPa (7 atm) process pressure at a wall temperature of 1050 K and the corrosive $\text{H}_2\text{SO}_4/\text{SO}_3/\text{H}_2\text{O}$ gases. Using the criteria of Mori (16), adequate creep rupture strength (<1% creep in 20 years) at 12 MPa (1760 psi) can be provided using a 5 cm wall.

The cost of the SiC heating elements would be around \$1.7 million. The cost of these vessels can be estimated, using the Peters and Timmerhaus method (17) and based on a bare reactor vessel weight of 15 Mg (33,000 lb). The cost was estimated at \$100,000 each, fabricated out of Incoloy 800 (similar to 304 SS). Installation of floating headers and the SiC heating elements are expected to double the bare vessel cost to \$1.7 million, bringing the total to \$18.7 million. Using the "Lang method" (18) we arrive at a fixed capital investment of \$80 million including installation, instrumentation, piping, electrical, services, etc.; and engineering, contingencies, fees, etc. This is equivalent to around 216/GJ of delivered energy.

Comparisons to our other SO_3 decomposer designs on the same economic basis are shown in Table 3. We have used the "Lang method" (17) where the fixed capital investment is around 4.28 times the purchase price of the equipment.

Impact on Cycle Efficiency

Although we have not finished the complete heat integration of the H_2SO_4 section of the cycle with the other sections of the cycle, we can put together a rough power systems flow diagram as in Fig. 10. The major heat demand process units are found in the H_2SO_4 section, and the heat demands and electrical loads are consistent with our most current design concepts. The loads for the other sections are taken as identical to those presented on the 1978 G.A. cycle Flowsheet (4), with the exception of the H_2/I_2 distillation which is based on their very recent G.A. advances in process chemistry. There will be further shifts in the heat

Table 3. Cost Comparison with Our Other SO_3 Decomposer Concepts.^a

Concept	Investments		Contribution to Energy Cost \$/GJ
	Fabricated Cost \$M	of Fixed Capital \$M	
Packed Bed	150	642	225
Fluidized Bed			
Sodium	32.8	140	49
Helium	52.7	224	78
Catalytic: Cartridge			
Axial-Flow	46	197	69
Cross-Flow	26	111	39
Joule-Boosterd	18.7	80	28

^aBasis: 85% stream factor, 12% interest (I), zero equity, 20 year plant life (L), 3000 MW_t TMR, H_2 production at 4927 $\text{gmol H}_2/\text{s}$ or 110 SM^3/s or 397,000 SM^3/h , energy production rate = 1.404 GJ/s at 47% cycle efficiency.

$$\text{Annualized cost, } A = \frac{(1+I)^L}{(1+I)^L - 1} \times \text{Fixed Capital Investment}$$

$$\text{Contribution to energy cost} = \frac{L \times A}{\text{Energy Produced Over Life}}$$

Accuracy of Costs: $\pm 50\%$

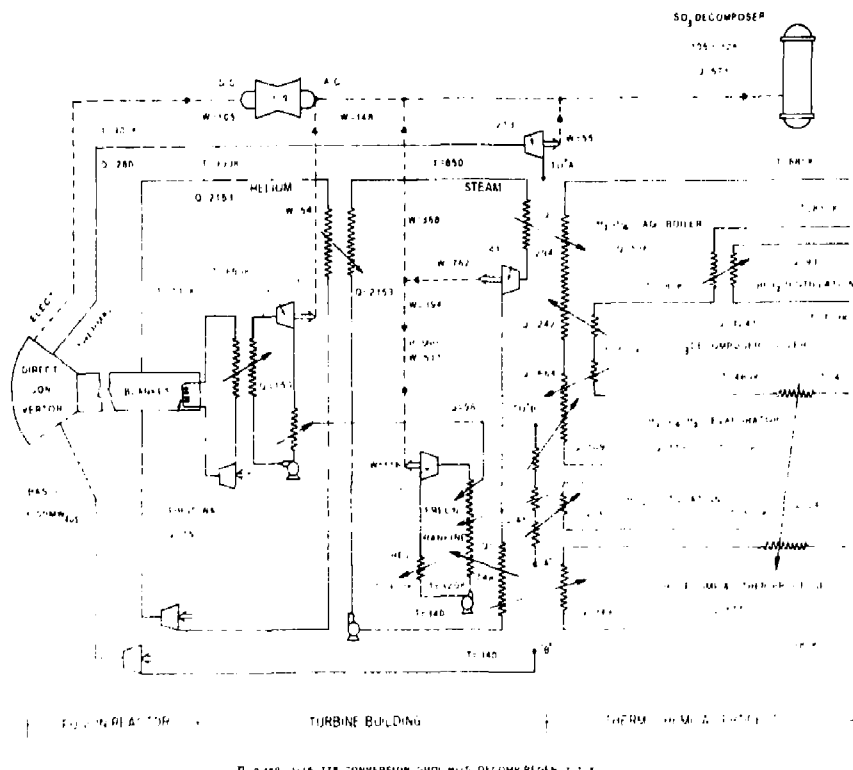


Fig. 10. Power systems configuration.

loads at several locations in the process, but they are expected to be minor. We have also assumed that around 320 K energy is rejected as low grade heat from the cycle. There are around 15% errors in closing this first cut heat balance.

For the base case we have assumed a TMR Q of 15 and a decomposer input temperature of 950 K. We can make a rough prediction of the cycle efficiency from these heat and electrical power flows in Fig. 10. The total energy supplied to the process by the TMR is taken as the sum of the direct converter dc and the thermal output from the first wall, direct converter and blanket heat exchangers and is found to be 2668 MW. The H₂ production higher heating value is 285.2 kJ/gmol H₂ or 1305 MW_t at 4580 gmol H₂/s thus, the cycle efficiency is calculated at around 48.9%. This is the highest cycle efficiency obtained for this base case after a large number of efforts to configure the power systems with the minimum number of heat exchangers. It is apparent from this diagram that an effort was made to match up the temperature levels wherever possible and cascade the heat down to the lowest temperature levels in the process. Undoubtedly with further insight, small improvements can be made on this base case.

We have also done some parametric sensitivity case studies to examine opportunities for further reductions in cost. Some of the most significant cases are summarized in Fig. 11. Clearly the most important parameter is the TWR Q , since an increase from $Q = 15$ to

$Q = 25$ increases cycle efficiency about 3%. If easing the decomposer feed from 950 K to 1150 K increases the cycle efficiency about 2% we selected the lower temperature of 950 K as a "base case" since we feel the recuperating heat exchangers on the decomposer can conservatively be made from Incoloy 800H, which may tolerate an 1100 K wall with corrosive process gases at 7 atm. Some innovative design techniques may allow us to raise the temperature.

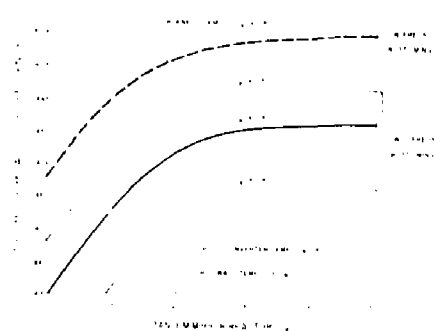


Fig. 11. Effect of TMR Q on cycle efficiency

Also shown in Fig. 11 is the effect of removing the freon bottoming cycle and varying the blanket temperature. We have not as yet costed out the bottoming cycle, but suspect that the minimum cost plant may be achieved by operating the blanket helium at 1000 K and eliminating the bottoming cycle.

Also explored were cases for the cogeneration of H₂ and electricity for the grid. Cogeneration capitalizing on the unique features of the TMR direct converter appears really significant.

CONCLUSIONS

1. The Joule-heated SO₃ decomposer can be operated at 1250 K from available ac power from the direct converter and the blanket.
2. Silicon carbide heating elements are economically attractive and are believed to have compatible material properties for the H₂SO₄/H₂O system. They need not be catalytically active.
3. The Joule-boosted decomposer is a more compact and less expensive unit than any of the earlier concepts of packed bed, fluidized bed, or catalytic cartridge decomposer reactors.
4. The Joule-boosted decomposer offers the best possible safety isolation of the SO₂/O₂/H₂O process gases from the liquid metal-containing blanket.
5. We have been able to develop a power-flow system layout that provides for utilization of various heat supplies and demands in order to obtain a cycle efficiency of around 49% with a low TMR Q = 15, 900 K helium from the blanket, a decomposer feed stream at 950 K, and a freon bottoming cycle.
6. Increasing Q to 25 raises cycle efficiency to around 51%.

ACKNOWLEDGEMENTS

Much of this work would not be possible without my colleagues Dick Werner and Oscar Krikorian, Lawrence Livermore National Laboratory; Professor Mike Hoffman, University of California at Davis; Don Rowe of Rowe Associates; and Professors Fred Ribe and Gene Woodruff of University of Washington.

We gratefully acknowledge the wonderfully cooperative efforts of Gottfried Besenbruch, John Norman, Ken McCorkle, Ken Schultz, Paul Trester and Lloyd Brown of General Atomic Company.

REFERENCES

1. T. R. Galloway and R. W. Werner, "Some Chemical Engineering Challenges On Driving Thermochemical Hydrogen Processes with the Tandem Mirror Reactor," 73rd Meeting of the American Institute of Chemical Engineers, Chicago, Illinois, November 10-20, 1980, and Lawrence Livermore National Laboratory, Tech. Rept. UCRL-84630, November 10, 1980.
2. R. W. Werner, Editor, "Synfuels from Fusion-Producing Hydrogen with the Tandem Mirror Reactor --and Thermochemical Cycles," Lawrence Livermore National Laboratory, Rept. UCID-18909, Vols. I and II, Jan. 21, 1981; plus private communications with Dick Werner and Oscar Krikorian, February 1981, Lawrence Livermore National Laboratory.
3. T. R. Galloway, "Some Process Aspects of Hydrogen Production Using the Tandem Mirror Reactor," 4th American Nuclear Society Topical Meeting, King of Prussia, PA, October 14-17, 1980, and Lawrence Livermore National Laboratory, Rept. UCRL-84285, October 8, 1980.
4. K. McCorkle, et al., "Development of a Sulfur-Iodine Thermochemical Water-Splitting Cycle for Hydrogen Reduction," 14th Intersociety Energy Conversion Engineering Conference, Proceedings, pp. 737-742, American Chemical Society, August 1979.
5. T. R. Galloway, "Interfacing the Tandem Mirror Reactor to the Sulfur-Iodine Process for Hydrogen Production," 15th Intersociety Energy Conversion Engineering Conference, August 8-22, 1980, Seattle, Washington, and Lawrence Livermore National Laboratory, Rept. UCRL-84212, June 2, 1980.
6. J. P. Pierre and R. L. Ammon, Westinghouse Co., Pittsburgh, PA, private communication, December, 1979.
7. H. Fedders, K. Hammelke, and E. Savvidis, Institut für Reaktor Studies, Jülich, Germany, private communication, December, 1979.
8. D. R. O'Keefe, J. H. Norman, and D. G. Williamson, "Catalysis Research in Thermo-Chemical Water-Splitting Processes," Rept. GA-A15722, General Atomic Company, January, 1980.
9. J. H. Norman, K. J. Mysels, R. Shipp, and D. Williamson, "Studies of the Sulfur-Iodine Thermo-Chemical Water-Splitting Cycle," Rept. GA-A15757, General Atomic Company, February, 1980.
10. K. R. Schultz, "Lee Rovner's Back-Reaction Calculations," General Atomic Company (private communication, FDAT/80-17), May 8, 1980.
11. D. Van Velzen, H. Langenkamp, G. Schuetz, D. Lalonde, J. Flamm, and P. Fiebeleman, "Development and Design of a Continuous Laboratory-Scale Plant for Hydrogen Production by the Mark-13 Cycle," Int-J-Hydrogen Energy 5, pp. 131-139 (1980).
12. L. Brown, General Atomic Co., private communication, December 22, 1980.
13. O. H. Krikorian, Lawrence Livermore National Laboratory, private communication, December 24, 1980.
14. E. R. G. Eckert and R. M. Drake, "Heat and Mass Transfer," McGraw-Hill, New York, 1959.
15. E. R. G. Eckert and R. M. Drake, "Analysis of Heat and Mass Transfer," McGraw-Hill Book Co., 1972.
16. Y. Mori, "Performance of Heat Exchangers on HTGR Application," ASME prep.int. 80-HT-39, Nat'l Heat Transfer Conference, Orlando, Florida, July 27-30, 1980.
17. M. S. Peters, K. D. Timmerhaus, "Plant Design and Economics for Chemical Engineers," McGraw-Hill, Book Co., 1980.